

# 1 mrangr: An R package for mechanistic simulation of metacommunities

2 Katarzyna Markowska<sup>\*1</sup>, Michał Wawrzynowicz<sup>1</sup>, Lechosław Kuczyński<sup>1</sup>

3 <sup>1</sup> Population Ecology Lab, Faculty of Biology, Adam Mickiewicz University, Uniwersytetu

4 Poznańskiego 6, 61-614 Poznań, Poland

5 \* Corresponding author: [katarzyna.markowska@amu.edu.pl](mailto:katarzyna.markowska@amu.edu.pl)

## 6 ORCID's

7 Katarzyna Markowska 0000-0001-5646-4611

8 Michał Wawrzynowicz 0009-0001-3729-3439

9 Lechosław Kuczyński 0000-0003-3498-5445

## 10 Abstract

11 1. Metacommunity theory unifies ecology by integrating local biotic interactions with regional  
12 dispersal and environmental filtering. However, testing theoretical predictions against  
13 empirical data remains challenging due to the difficulty of disentangling these processes in  
14 nature and the confounding effects of imperfect detection.

15 2. Here, we introduce `mrangr`, an R package designed for the mechanistic, spatially explicit  
16 simulation of multispecies communities. Unlike correlative approaches, `mrangr` strictly  
17 distinguishes between the fundamental niche (determined by abiotic carrying capacity) and  
18 the realised niche (an emergent property of biotic interactions).

19 3. The package implements a generalized Lotka-Volterra framework on a lattice grid (via the  
20 `terra` ecosystem), allowing users to simulate diverse interaction types — including  
21 competition, predation, and facilitation — alongside species-specific dispersal kernels.  
22 A defining feature is the "Virtual Ecologist" module, which samples the simulated "ground

23 "truth" with user-defined observation errors and sampling designs, thereby mimicking the  
24 constraints of real-world biodiversity surveys.

25 4. We demonstrate the package's capabilities through three case studies: (i) quantifying the  
26 scale-dependent effects of dispersal on  $\alpha$ ,  $\beta$ , and  $\gamma$  diversity, (ii) testing the conditions under  
27 which the competition-colonization trade-off promotes coexistence in the presence of fitness  
28 inequalities, and (iii) assessing the recoverability of fundamental niches from imperfect  
29 observational data constrained by biotic interactions.

30 5. By providing a flexible platform to generate synthetic data with known underlying  
31 mechanisms, `mrangr` enables researchers to benchmark statistical models, assess sampling  
32 strategies, and rigorously test hypotheses at the interface of theoretical and empirical  
33 macroecology.

34

35 **Key-words:** metacommunity dynamics, fundamental and realized niche, community assembly,  
36 process-based modelling, virtual ecologist, spatially explicit

37 **Running Head:** Mechanistic metacommunity simulation in R

38 **1. Introduction**

39 One of the key goals of ecology is to understand the mechanisms generating and maintaining  
40 biodiversity. Traditionally, theory separated these mechanisms by spatial scale: regional frameworks  
41 emphasized ecological drift, selection, speciation, and dispersal (Vellend, 2016), whereas local models  
42 focused on competitive coexistence (Chesson, 2000), and priority effects (Adler et al., 2007; Ke &  
43 Letten, 2018). Metacommunity theory (Leibold et al., 2004, 2017) unifies these perspectives by  
44 identifying three spatially explicit mechanisms that operate across scales: density-independent  
45 responses to abiotic conditions, density-dependent biotic interactions, and dispersal (Thompson et  
46 al., 2020).

47 While explicitly integrating these mechanisms is essential for unravelling biodiversity patterns, a  
48 critical limitation of many existing metacommunity tools is the conflation of the fundamental and  
49 realized niche. Frequently, simulators rely on input suitability maps that implicitly incorporate biotic  
50 constraints, rendering it impossible to disentangle environmental filtering from community processes.  
51 To overcome this, a mechanistic framework must strictly define the fundamental niche as a measure  
52 of environmental potential, allowing the realized niche to emerge purely as a dynamic property of  
53 biotic interactions and dispersal.

54 Against this requirement for mechanistic clarity, the current landscape of process-based  
55 metacommunity simulators – namely `gen3sis` (Hagen et al., 2021) and `metaIBM` (Lin et al., 2024)  
56 - often necessitates trade-offs. While these frameworks share a core principle of coupling dispersal  
57 and density-dependent regulation, they implement interspecific regulation indirectly by the  
58 magnitude of fundamental niche overlap. This reliance on overlap prevents the explicit modelling of  
59 metacommunities with asymmetric (e.g. predation) or positive (e.g. facilitation) interactions,  
60 effectively locking the simulation into the "conflated niche" paradigm. Conversely, `metaRange`  
61 (Fallert et al., 2025) provides a programming environment in which multiple processes, including all  
62 types of biotic interactions, can be modelled flexibly; yet users must code these functionalities

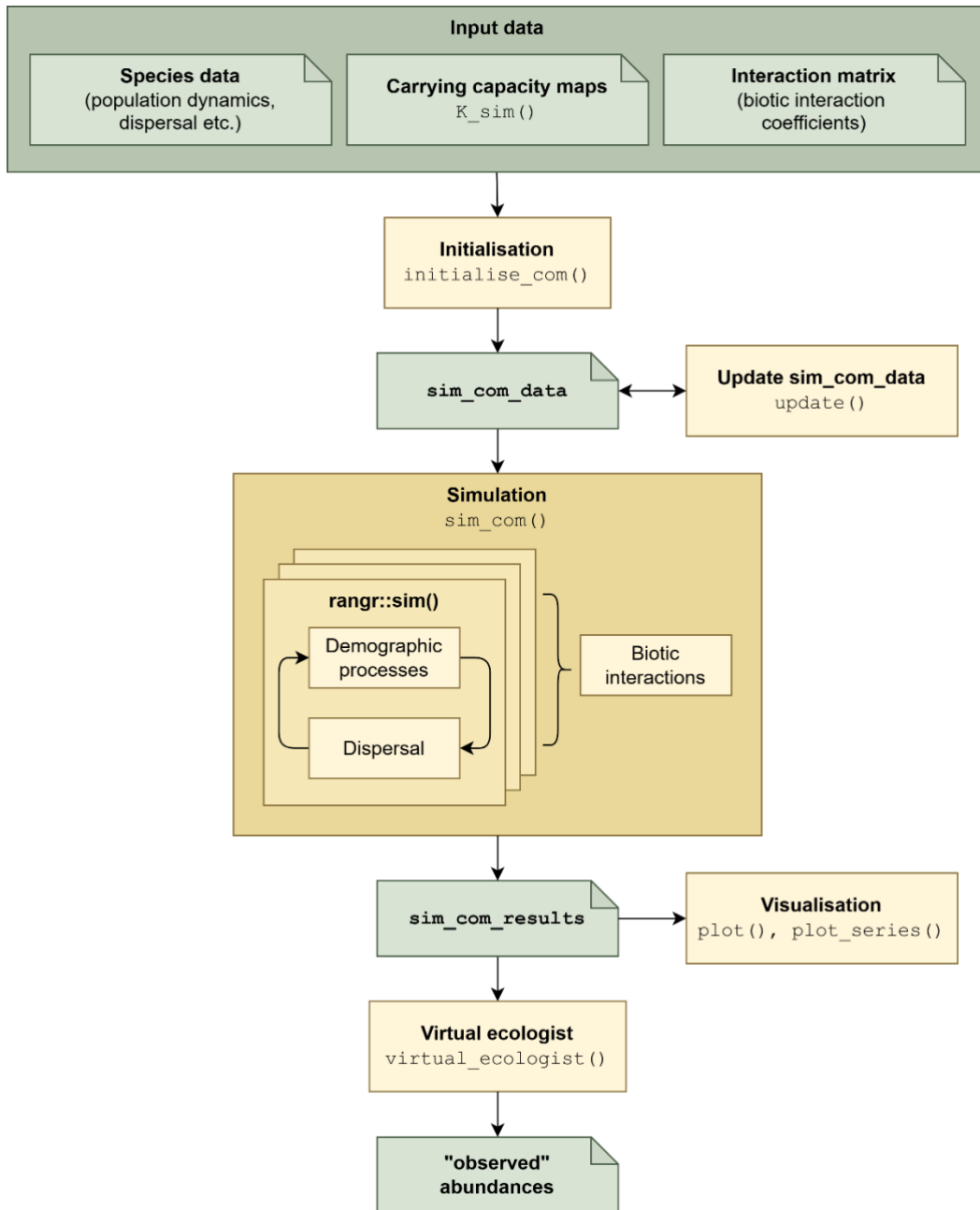
63 themselves. Consequently, no off-the-shelf tool is currently capable of simulating metacommunities  
64 with flexible, asymmetric biotic interactions while maintaining a strict separation between abiotic and  
65 biotic drivers.

66 To address this gap, we have developed `mrangr`: an R package for flexible, mechanistic  
67 metacommunity simulation in which dispersal processes, demographic rates and biotic interaction  
68 coefficients can be explicitly parametrised. Built as a multi-species extension of the `rangr` package  
69 (Markowska et al., 2025), `mrangr` inherits that tool's accessible parameterisation of population  
70 dynamics, dispersal, and virtual ecology. By representing species relationships through an asymmetric  
71 interaction matrix, it enables the simulation of diverse biotic interactions — including competition,  
72 facilitation, and predation — within a spatially explicit virtual environment. Moreover, by defining the  
73 fundamental niche strictly through user-supplied carrying capacity maps, the package allows the  
74 realized niche to emerge dynamically. This separation enables researchers to quantify the 'biotic  
75 deficit' - the specific loss of range or abundance attributable solely to biotic interactions - by comparing  
76 the input carrying capacity maps against the simulated equilibrium state.

## 77 2. Package overview

78 The core architecture of `mrangr` is designed to mechanistically decouple the fundamental niche from  
79 the realized niche (Figure 1). Users define the environmental potential for each species via spatially  
80 explicit carrying capacity maps ( $K$ ) and intrinsic growth rates ( $r$ ), while biotic constraints are governed  
81 by a user-supplied asymmetric interaction matrix ( $a$ ). Consequently, the realized metacommunity  
82 emerges dynamically from the interplay of species-specific demography, dispersal constraints, and  
83 pairwise interactions. To bridge the gap between these theoretical mechanisms and empirical reality,  
84 the package includes a 'virtual ecologist' module that replicates both observation error and the specific  
85 sampling designs of biological surveys. Crucially, this module generates outputs that mimic the  
86 structure of empirical monitoring data, such as sparse spatiotemporal records rather than complete

87 grids. This structural fidelity allows researchers to feed simulated datasets directly into standard  
88 analytical pipelines (e.g., SDMs or occupancy models), providing a rigorous platform for benchmarking  
89 statistical methods against a known ground truth. A comprehensive overview of the supported  
90 biological and observational processes is provided in Table 1.



91

92 Figure 1. Conceptual framework and operational workflow of the `mrangr` package. The schematic  
 93 illustrates the mechanistic decoupling of drivers: the fundamental niche is strictly defined by input  
 94 carrying capacity maps, while the realized niche emerges dynamically from the integration of biotic  
 95 interactions, demographic rates, and dispersal. The workflow progresses from initialization to the  
 96 'virtual ecologist' module, which simulates observational errors. Green rectangles represent data  
 97 objects (inputs and state variables), while yellow rectangles represent the package's core functions  
 98 governing metapopulation dynamics and sampling.

99 Table 1. Overview of the `mrangr` framework, distinguishing between the ecological state processes  
 100 (mechanisms generating the true abundance) and the observation model (mechanisms generating  
 101 survey data).

Simulation Component	Impact	Implementation in <code>mrangr</code>
<b>PROCESS MODEL</b>		
Abiotic constraints (Fundamental niche)	Defines the potential range and maximum abundance of a species based solely on environmental physiology, ignoring other species.	Users supply carrying capacity maps ( $K$ ), either as static rasters or generated dynamically via <code>K_sim()</code> based on environmental variables.
Biotic filtering (Realized niche)	Modifies the fundamental niche by reducing abundance (competition, predation) or expanding it (facilitation), creating the realized distribution.	The interaction matrix ( $a$ ) defines pairwise coefficients. The simulation solves for abundance at each time step, allowing the realized niche to emerge dynamically from the $K$ maps and matrix $a$ .
Dispersal	Regulates connectivity. Low rates cause dispersal limitation, preventing species from reaching suitable patches. High rates drive mass effects (source-sink dynamics) and rescue effects.	Users control the spread via the <code>kernel_fun</code> parameter in <code>initialise_com()</code> . This allows for modelling constrained diffusion (limitation) or fat-tailed distributions (long distance dispersal) to simulate different isolation scenarios.
Ecological drift	Stochastic changes in abundance, dominant in small populations.	Demographic stochasticity is inherent to the simulation. Additional noise can be introduced into demographic rates or environmental layers using <code>initialise_com()</code> or <code>update()</code> functions.
<b>OBSERVATION MODEL</b>		
Observation process	Distorts biological patterns through sampling bias and imperfect detection. Essential for validating analytical methods against "known" truths.	The <code>virtual_ecologist()</code> function samples the simulated metacommunity. Users can specify sampling designs (e.g., random, systematic) and detection probability distributions (e.g., <code>obs_error</code> ) to generate realistic "observed" datasets.

102 3. Key features of the package

103 `mrangr` inherits the core population dynamics of `rangr`, including spatially explicit growth models,  
104 flexible dispersal kernels, and non-monotonic regulation (e.g., Allee effects). As these fundamental  
105 mechanisms are detailed in Markowska *et al.* (2025), we focus here on the novel functionalities  
106 emerging from their integration into a multi-species context.

107 3.1. Interspecific regulation

108 Central to `mrangr` is a generalized interaction matrix that enables the simulation of diverse  
109 community dynamics. By parameterising both positive and negative coefficients in an  
110 asymmetric matrix ( $a$ ), users can represent a full spectrum of ecological interactions, including  
111 competition, facilitation, and predation.

112 Biotic interactions are modelled via a square numeric matrix where each element  $a_{ij}$   
113 represents the *per-capita* interaction strength of species  $j$  on species  $i$ . Mechanistically, this  
114 coefficient defines the change in the carrying capacity of species  $i$  caused by a single individual  
115 of species  $j$ . Consequently, the realized niche is calculated dynamically: at each time step, the  
116 effective carrying capacity of a focal species is derived by modifying its fundamental niche  
117 ( $K_{fund}$ ) by the net biotic influence of the community.

118 Formally, the effective carrying capacity for species  $i$  at time  $t$  in a given cell is calculated as:

$$119 K_{i,t} = \max \left( K_{i,fund} + \sum_{j=1}^S (a_{i,j} \cdot N_{j,t-1}), 0 \right)$$

120 where  $S$  is the total number of species,  $N_{j,t-1}$  is the abundance of species  $j$  at the previous  
121 time step, and the  $\max(\dots, 0)$  function ensures that carrying capacity remains non-negative.  
122 This formulation represents a specific implementation of the Lotka-Volterra framework where  
123 interactions expand or contract the available niche space ( $K$ ) rather than acting directly on  
124 intrinsic growth rates ( $r$ ).

### 3.2. Low entry level

The package is designed to minimize technical complexity, requiring only two primary functions to execute a complete simulation. First, a community object is established using the `initialise_com()`, which integrates spatial carrying capacity maps ( $K$ ), the biotic interaction matrix ( $a$ ) and species-specific life-history parameters. Subsequently, the `sim_com()` function executes the spatially explicit simulation. This streamlined workflow reduces the programming workload, allowing ecologists to study complex feedback loops and metacommunity dynamics without having to create custom simulation engines.

### 3.3. Invasion dynamics

The package offers specialised functionality to simulate species invasions. Users can designate specific species as invaders and schedule their introduction at defined time steps, rather than initializing them at the start of the simulation. This temporal flexibility enables the mechanistic investigation of invasion success. It allows researchers to explore how community composition, biotic resistance and arrival timing shape the settlement of new species within established metacommunities.

### 3.4. Virtual ecologist

A major challenge in ecology is that theoretical models often assume perfect knowledge, whereas empirical data is inherently noisy and incomplete. To bridge this gap, `mrangr` includes a Virtual Ecologist module designed to replicate the constraints of real-world biological surveys. While the simulation inherently generates "true" abundances (perfect knowledge), the `virtual_ecologist()` function allows users to filter this output through imperfect observation methods. The module supports:

- Sampling designs: Users can define the sampling intensity (e.g., surveying only 5% of the landscape) and spatial configuration (random vs. systematic sampling).

- Detection error: This involves simulating imperfect detection and observation bias by applying error distributions (e.g. Binomial to mimic imperfect detectability or log-Normal to impose observation error on counts) to true abundance data.

By generating "observed" datasets alongside known ground truths, this feature allows researchers to rigorously benchmark statistical methods (such as species distribution models or occupancy models) and quantify how sampling limitations affect ecological inference.

### 3.5. Virtual environment generator

To facilitate theoretical investigations, the `K_sim()` function allows for the generation of spatially explicit carrying capacity maps based on spatially autocorrelated Gaussian Random Fields (GRFs). This tool enables users to construct controlled synthetic landscapes by defining both the spatial structure (via the autocorrelation range) and the statistical properties (marginal distributions) of the environment. Furthermore, the function supports the specification of cross-correlations between different landscape layers, allowing researchers to simulate complex niche relationships — such as environmental trade-offs or positive associations — under precise experimental conditions. This offers a versatile framework for testing ecological hypotheses across a range of environmental configurations.

### 3.6. GIS integration

Unlike theoretical tools that rely solely on synthetic landscapes, `mrangr` is fully integrated with the `terra` ecosystem, the modern standard for spatial data analysis in R (Hijmans, 2026). This interoperability allows users to directly ingest empirical raster data — such as climate layers, land cover maps, or remote sensing outputs — to define simulation arenas. By enabling the use of real-world geographical data as boundary conditions, `mrangr` facilitates the seamless transition from abstract theoretical exploration to data-driven macroecological modelling.

173        3.7. Computational efficiency

174        Spatially explicit simulations are often computationally expensive, particularly when scaling

175        up to large landscapes or high species richness. `mrangr` addresses this by delegating

176        intensive spatial operations to the `terra` package, which is optimized in C++. This allows the

177        package to maintain the flexibility and readability of pure R code while achieving the

178        performance necessary to handle large landscape grids and extensive replication.

179        Furthermore, the package is designed to support parallel execution. As demonstrated in the

180        provided case studies, users can easily distribute replicates across processor cores using

181        standard R parallelization tools (e.g., `parallel`, `pbapply`), making it feasible to conduct

182        extensive sensitivity analyses and robustly estimate parameter uncertainty.

## 183        4. `mrangr` workflow

184        The `mrangr` package provides a straightforward workflow consisting of 3 main steps.

### 185        4.1. Environment and community initialisation

186        The workflow begins by defining the simulation arena and the community structure. Users can

187        integrate empirical spatial data by providing `SpatRaster` objects for carrying capacity maps ( $K$ ),

188        representing species fundamental niches, and initial abundance maps ( $N_1$ ). Alternatively, for

189        theoretical applications or sensitivity testing, the `K_sim()` function allows users to generate

190        synthetic, spatially autocorrelated carrying capacity landscapes. Concurrently, interspecific

191        dynamics are parameterised via an asymmetric interaction matrix ( $a$ ), enabling the representation

192        of complex biotic relationships. The `initialise_com()` function integrates the spatial data

193        and interaction parameters into a `sim_com_data` object. At this stage, users define species-

194        specific traits, including intrinsic growth rates ( $r$ ) and dispersal kernels (`kernel_fun`). This step

195        validates the input maps and community parameters before the simulation begins, while also

196        encapsulating all this data into a single `sim_com_data` object.

197 4.2. Simulation execution

198 Once the system is defined, the `sim_com()` function executes the spatially explicit simulation  
199 over discrete time steps. In each iteration, the model sequentially resolves dispersal and local  
200 population dynamics. First, the effective carrying capacity ( $K_{i,t}$ ) of every grid cell is dynamically  
201 updated based on the local abundance of all interacting species (as defined by the interaction  
202 matrix  $\alpha$ ). Populations then grow according to their intrinsic growth rates ( $r$ ), constrained by these  
203 dynamically updated realized niches. Simultaneously, individuals disperse across the landscape  
204 according to species-specific kernels. This cycle repeats for the specified duration, generating a  
205 complete spatiotemporal history of the metacommunity that captures the interplay between  
206 environmental forcing, biotic interactions, and dispersal.

207 4.3. Observation and analysis

208 Following the simulation, users can analyse the "biological truth" directly or, optionally, pass the  
209 results to the `virtual_ecologist()` function. This post-processing step applies the  
210 observation constraints described in [Section 3.4](#) to the raw simulation output. By defining specific  
211 sampling protocols (e.g., plot number, detection probability) at this stage, users generate an  
212 "observed" dataset derived from the "true" state. This dual-output workflow allows researchers  
213 to seamlessly benchmark analytical methods by comparing statistical inferences drawn from the  
214 virtual samples against the known ground truth of the metacommunity. Following the simulation  
215 (and optionally an observation process), the resulting community state can be analysed directly.  
216 The package provides native plotting methods: `plot_series()` generates temporal  
217 trajectories of total or mean abundance for all species, while `plot()` visualises the spatial  
218 distribution (i.e. realised niches) of the metacommunity at specific time points.

219 **5. Case studies**

220 We present three case studies to validate the simulator against established ecological theory. The first  
221 two examples benchmark `mrangr` against known biological patterns: the influence of dispersal on  
222 biodiversity scaling and the dynamics of competition-colonization trade-offs. The third example  
223 demonstrates the package's methodological utility, evaluating the limitations and potential of  
224 inferring fundamental niches from observation-based data.

225 The three case studies were run in the same exemplary simulation environment, defined on a 20×20  
226 grid (400 cells) with a 1 km resolution, assuming a coordinate system EPSG:2180. Trends in simulated  
227 parameters were quantified and visualised using Generalized Additive Models for Location, Scale and  
228 Shape (GAMLSS) to capture non-linear responses and heteroscedasticity.

229 **5.1. Example 1: Testing the effect of dispersal on species diversity**

230 Dispersal is the fundamental process connecting local communities, shaping biodiversity patterns at  
231 multiple scales. In metacommunity theory, dispersal promotes local coexistence through the rescue  
232 effect, yet potentially undermines regional diversity by homogenizing distinct communities (Mouquet  
233 & Loreau, 2003). Consequently, the relationship between dispersal ability and diversity metrics is  
234 expected to vary across scales. Increased dispersal should theoretically elevate local richness  
235 ( $\alpha$ -diversity) by overcoming dispersal limitation, while simultaneously eroding compositional turnover  
236 ( $\beta$ -diversity) through mass effects. At the regional scale ( $\gamma$ -diversity), these opposing forces may  
237 generate a unimodal response, where biodiversity peaks at intermediate dispersal rates that balance  
238 colonization against competitive exclusion. Testing these predictions empirically is challenging due to  
239 the difficulty of manipulating dispersal traits. Here, we demonstrate how `mrangr` can be used to  
240 rigorously test these macroecological hypotheses by simulating metacommunities across a controlled  
241 gradient of dispersal ranges while keeping niche requirements and interaction strengths constant.

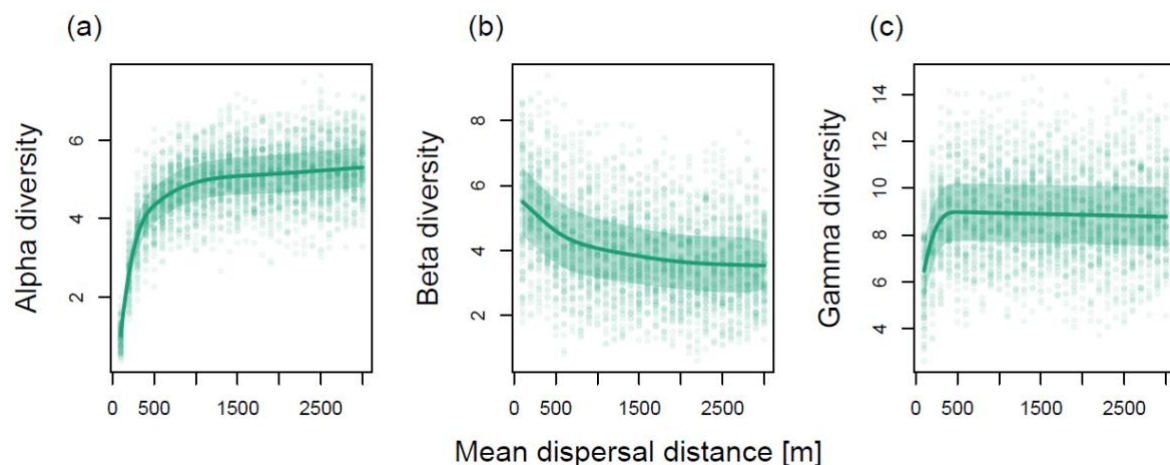
242 In this example, the metacommunity consisted of 20 species. For each simulation replicate,  
243 species-specific carrying capacity maps ( $K$ ) were generated using spatially autocorrelated log-normal  
244 distributions. Biotic interactions were modelled via an asymmetric interaction matrix ( $a$ ) with  
245 coefficients drawn from a normal distribution. The experimental gradient focused on dispersal ability.  
246 We varied the mean dispersal distance from 100 m to 3000 m across 30 discrete intervals. Dispersal  
247 was modelled using an exponential kernel, where the rate parameter is defined as  $1/\text{mean}$  distance.  
248 We performed 100 independent replicates for each dispersal scenario. Each simulation ran for 20 time  
249 steps, sufficient to allow the metacommunity to reorganize from its initial state under the imposed  
250 dispersal and interaction constraints. At the final time step, we calculated diversity metrics based on  
251 Hill numbers with  $q = 1$  (exponential of Shannon entropy):

- 252 1. Alpha diversity ( $\alpha$ ): calculated as the mean local diversity across all 400 grid cells.
- 253 2. Gamma diversity ( $\gamma$ ): calculated based on the total pooled abundance of each species across  
254 the entire landscape.
- 255 3. Beta diversity ( $\beta$ ): derived using additive partitioning:  $\beta = \gamma - \alpha$ .

256 The simulation results confirm the opposing effects of dispersal on biodiversity across spatial scales,  
257 reproducing classic theoretical predictions (e.g., Mouquet & Loreau, 2003):

- 258 1. Local enrichment ( $\alpha$ -diversity): As predicted, local species richness increased monotonically  
259 with dispersal ability (Figure 2a). At low dispersal rates, local communities are impoverished  
260 due to local extinctions and dispersal limitation. Increasing connectivity allows species to  
261 colonize and persist in suboptimal patches ('sink' habitats) via the rescue effect, thereby  
262 inflating local diversity.
- 263 2. Spatial homogenization ( $\beta$ -diversity): Conversely, compositional turnover declined sharply as  
264 dispersal increased (Figure 2b). High dispersal rates effectively mix the metacommunity,  
265 eroding the spatial distinctions driven by environmental heterogeneity.

266 3. The regional trade-off ( $\gamma$ -diversity): The response of regional diversity highlights the tension  
 267 between local enrichment and spatial homogenization (Figure 2c). Gamma diversity increases  
 268 rapidly at low dispersal distances as species overcome dispersal limitation, eventually  
 269 saturating at a stable plateau. Unlike simple theoretical models that predict a decline in  
 270 diversity at high dispersal rates due to global competitive exclusion, our results indicate that  
 271 spatial heterogeneity in carrying capacity provides sufficient refuge for inferior competitors.  
 272 In this high-dispersal regime, species sorting mechanisms allow species to efficiently track  
 273 their environmental optima without being displaced from the landscape entirely, maintaining  
 274 high regional diversity despite extensive mixing.



275  
 276 Figure 2. Response of metacommunity diversity components to mean dispersal distance. Scatterplots  
 277 display (a) alpha, (b) beta, and (c) gamma diversity for metacommunities simulated with a regional  
 278 pool of 20 species. Points represent individual simulation runs. Solid lines indicate the median and  
 279 shaded regions represent the interquartile range, modelled using a Gaussian Location-Scale GAM  
 280 (GAMLSS).

## 281 5.2. Example 2: Competition–colonization trade-off

282 A fundamental puzzle in community ecology is explaining how inferior competitors avoid exclusion in  
 283 landscapes dominated by superior species. The competition–colonization trade-off hypothesis

284 provides a classic metacommunity solution, proposing that species coexist by partitioning the  
285 landscape based on dispersal ability rather than resource use (Tilman, 1994). In this framework,  
286 inferior competitors persist as "fugitive species" by investing in superior colonization rates, allowing  
287 them to occupy vacant patches before slower-dispersing dominants arrive to displace them.  
288 Identifying this trade-off in empirical systems is often confounded by environmental heterogeneity  
289 and complex trait correlations. In this example, we use `mrangr` to simulate a test of this hypothesis  
290 by enforcing a strict constraint between competitive rank and dispersal distance, evaluating whether  
291 this trade-off alone is sufficient to maintain regional coexistence in a spatially explicit context.

292 In this example, the metacommunity consisted of just two virtual species. To isolate the effect of  
293 dispersal on coexistence, we controlled for environmental preferences by enforcing complete  
294 fundamental niche overlap. Both species were assigned identical spatial habitat requirements,  
295 differing only in their competitive fitness within that niche:

296 1. Species 1 (superior competitor): Assigned a baseline carrying capacity generated via a  
297 log-normal distribution.

298 2. Species 2 (inferior competitor): Assigned a carrying capacity 20% lower than Species 1, across  
299 the entire landscape.

300 3. Biotic interactions: We applied strong, symmetric competition between the species ( $\alpha = -1$ ).  
301 Under these conditions — identical fundamental niches and distinct fitness levels — theory  
302 predicts the deterministic exclusion of Species 2 by Species 1 in every grid cell.

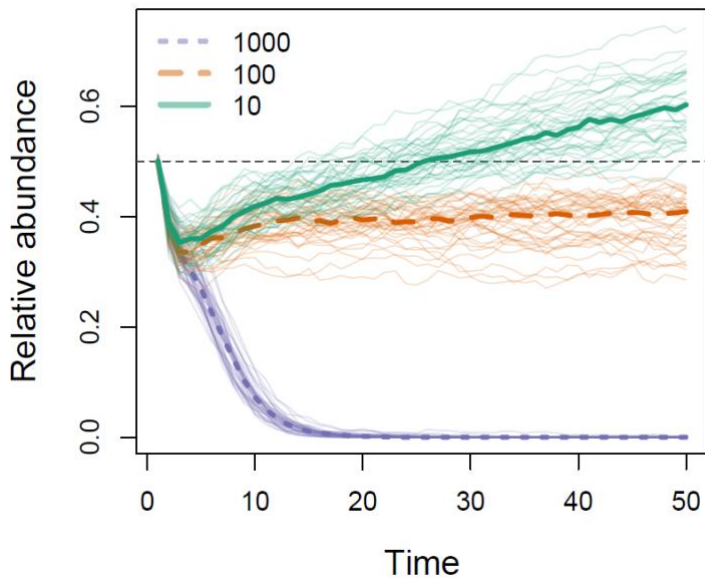
303 We introduced a trade-off where the inferior competitor (Species 2) compensated for its lower fitness  
304 with superior dispersal. We fixed the mean dispersal distance of Species 2 at 1000 m and  
305 systematically varied the mean dispersal of the superior competitor (Species 1) across three scenarios:

306 1. No trade-off (Control): Species 1 also disperses 1000 m (equal dispersal, unequal fitness).

307 2. Moderate trade-off: Species 1 disperses 100 m (10 $\times$  disadvantage).

308 3. Strong trade-off: Species 1 disperses 10 m (100 $\times$  disadvantage).

309 We performed 40 independent replicates per scenario over 50 time steps. We tracked the relative  
310 abundance of the inferior competitor to evaluate whether spatial niche partitioning (via colonisation  
311 ability) could prevent exclusion despite the lack of niche differentiation.



312

313 Figure 3. Testing the competition-colonization trade-off. Temporal dynamics of the inferior  
314 competitor's relative abundance over 50 simulation steps. The inferior competitor (Species 2) has a  
315 fixed high dispersal distance (1000 m) but lower competitive fitness ( $K_2 = 0.8 \times K_1$ ). Thin lines  
316 represent individual simulation trajectories (n=40), while thick lines indicate the median. Scenarios  
317 differ by the mean dispersal distance of the superior competitor (Species 1): 1000 m (violet, dotted  
318 line), 100 m (orange, dashed line), and 10 m (green, solid line).

319 The simulations demonstrate that dispersal advantage can effectively counteract competitive  
320 exclusion (Figure 3). In the absence of a trade-off, when both species shared equal dispersal  
321 capabilities (violet dotted line), the inferior competitor was rapidly driven toward extinction. However,  
322 as the trade-off strength increased, the inferior competitor's persistence improved significantly. In the  
323 strongest trade-off scenario (green solid line), where the superior competitor was severely dispersal-

324 limited (10 m), the inferior competitor successfully exploited vacant space, achieving numerical  
325 dominance despite its lower fitness.

326 **5.3. Example 3: Reconstruction of fundamental niches**

327 Estimating the fundamental niche from field data is complicated by two filters: biotic interactions,  
328 which constrain the realized distribution, and observational errors, which distort detection.  
329 Consequently, ecological field data rarely reflect pure environmental potential (Soberón, 2007). Yet,  
330 recovering this baseline is essential for forecasting species responses to novel environments. In this  
331 example, we use `mrangr` to simulate a known ground truth and systematically evaluate whether  
332 statistical models can penetrate these biological and observational layers to reliably reconstruct the  
333 fundamental niche.

334 Spatially autocorrelated environmental variables were generated using Gaussian Random Fields via  
335 the `K_sim()` function. The metacommunity consisted of 5 virtual species. For each species, the  
336 fundamental niche (carrying capacity,  $K$ ) was defined as a log-linear function of the environmental  
337 covariates, ensuring a known ground truth for species-environment relationships. To model the  
338 realized niche, we generated asymmetric interaction matrices ( $\alpha$ ) where off-diagonal elements were  
339 drawn from a normal distribution  $N(0, \delta^2)$ . We systematically varied the interaction strength  
340 parameter,  $\delta$ , across a gradient to simulate metacommunities ranging from purely abiotic-driven ( $\delta =$   
341 0) to highly interactive systems ( $\delta = 3$ ).

342 Simulations were initialized with abundances drawn from a Poisson distribution with expectations  
343 equal to the local carrying capacity ( $\lambda = K$ ). The system was evolved for 50 time steps, with the first  
344 10 steps serving as a burn-in period to allow the community to reach a quasi-equilibrium state. To  
345 replicate the spatiotemporal structure of empirical monitoring datasets, we employed the 'virtual  
346 ecologist' module across the subsequent 40 time steps. We sampled 10% of the available site-time  
347 combinations (`prop = 0.1`) and introduced observational error using a binomial distribution with  
348 detection probability  $p = 0.5$ , mimicking the imperfect detection typical of wildlife surveys.

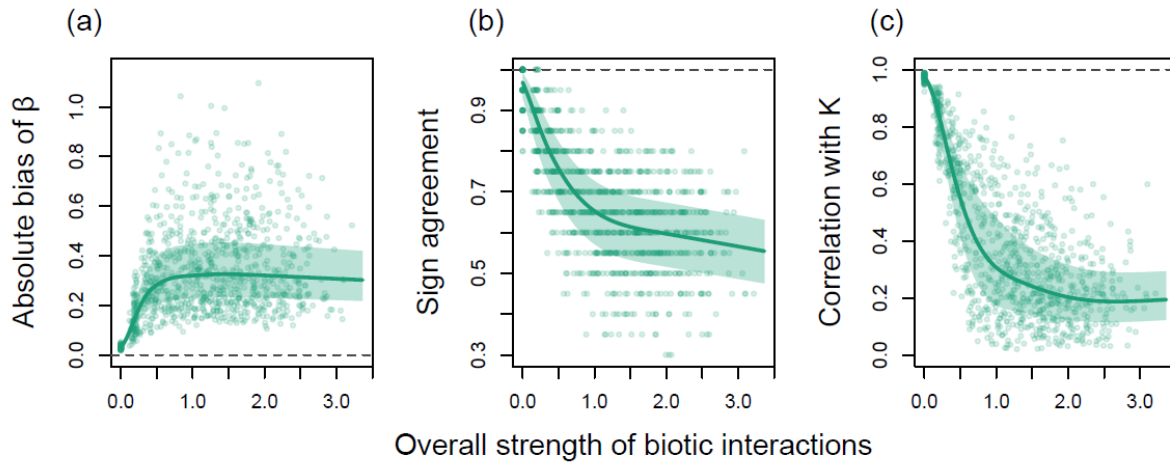
349 We attempted to reconstruct the fundamental niche from the sampled realized abundances using  
350 Generalized Linear Mixed Models (GLMMs) fitted via the `glmmTMB` package. The models included the  
351 true environmental covariates as predictors. We evaluated the performance of these reconstructions  
352 against the true fundamental niche ( $K$ ) using three metrics:

353 1. Bias of  $\beta$ : The absolute difference between the estimated environmental coefficient and the  
354 true coefficient used to generate  $K$ .

355 2. Sign agreement: The proportion of simulations where the model correctly identified the  
356 direction of the environmental response (positive/negative).

357 3. Correlation with  $K$ : The Spearman rank correlation between the spatially predicted  
358 abundance surface and the true carrying capacity map.

359 Our simulations demonstrate that interaction strength substantially impairs the statistical recovery of  
360 the fundamental niche. As the interaction strength increased, the spatial correlation between the  
361 reconstructed niche and the true carrying capacity declined non-linearly, effectively uncoupling  
362 realized abundance from environmental potential (Figure 4c). Concurrently, the absolute bias in  
363 estimated environmental coefficients ( $\beta$ ) rose (Figure 4a), indicating that biotic constraints  
364 systematically distort the perceived magnitude of environmental preferences. Most critically, under  
365 strong biotic regulation, the sign agreement dropped toward 0.5 (Figure 4b), equivalent to random  
366 guessing. This implies that in highly interactive communities, standard correlative models frequently  
367 misidentify positive environmental associations as negative (and vice versa), yielding spurious niche  
368 estimates driven by community dynamics rather than abiotic suitability.



369

370 Figure 4. Influence of biotic interaction strength on the accuracy of fundamental niche estimation by  
 371 the virtual ecologist. Interaction strength is defined as the mean absolute value of off-diagonal  
 372 elements in the interaction matrix. Estimation performance is evaluated via: (a) absolute bias of slope  
 373 estimates ( $\beta$ ); (b) sign agreement (proportion of estimated slopes matching the true sign); and  
 374 (c) correlation between estimated abundances and true carrying capacity ( $K$ ). Points represent  
 375 individual metacommunities. Solid lines indicate the median and shaded regions represent the  
 376 interquartile range, modelled using a Gaussian Location-Scale GAM (GAMLSS). Dashed horizontal lines  
 377 indicate reference values for optimal performance (zero bias or perfect agreement/correlation).

378 **6. Conclusions**

379 The metacommunity concept has traditionally been categorized into four major paradigms: species  
 380 sorting, mass effects, patch dynamics, and neutral theory (Leibold et al., 2004). While recent  
 381 theoretical work has moved toward a unified process-based metacommunity framework,  
 382 operationalization of this synthesis in a flexible simulation environment remains a challenge. Here, we  
 383 address this by conceptually reducing metacommunity dynamics into three axes—space, time, and  
 384 species—linked by fundamental ecological processes. Specifically, `mrangr` integrates population  
 385 growth (temporal dynamics), dispersal (spatial dynamics), and biotic interactions (interspecific  
 386 dynamics).

387 Although this abstraction is necessarily simplified, `mrangr` captures both the biotic interactions that  
388 drive local species coexistence, and the spatio-temporal population dynamics that determine  
389 community assembly while allowing for mechanistic flexibility. Crucially, this flexibility is grounded in  
390 the decoupling of the fundamental and realized niche. By defining environmental potential and biotic  
391 interactions as distinct, independent inputs, the package ensures that the realized niche emerges  
392 dynamically from their interplay rather than being an implicit artifact of suitability maps. Furthermore,  
393 incorporating stochasticity into each process enables the generation of parameter distributions from  
394 replicated simulations, facilitating robust statistical inference.

395 `mrangr` provides a user-friendly and flexible framework for spatially explicit metacommunity  
396 simulation. Its distinguishing features include support for arbitrary biotic interaction structures, fully  
397 spatially explicit environments, and an integrated observation process model. This enables precise  
398 mechanistic control over the primary processes driving community dynamics, allowing researchers to  
399 replicate established patterns while exploring complex frontiers—such as the disentanglement of  
400 abiotic filtering from competition, the interplay between niche and fitness differences, or the  
401 spatiotemporal dynamics of species invasions.

## 402 7. Authors' contributions

403 KM and LK conceived the ideas and designed the methodology; KM and LK developed the algorithm;  
404 KM led the software development and R package implementation; KM, MW, and LK wrote the  
405 documentation and vignettes; MW contributed to the validation and testing of the software. All  
406 authors contributed equally to the writing of the manuscript and gave final approval for publication.  
407 LK acquired the funding and provided overall supervision for the project.

408 **8. Acknowledgements**

409 The study was supported by the National Science Centre (NCN) in Poland (grant no.  
410 2018/29/B/NZ8/00066). The computational resources supporting this work were provided by the  
411 Poznań Supercomputing and Networking Centre (PCSS) (grant no. pl0090-01).

412 **9. Conflict of interest statement**

413 The authors declare no conflicts of interest.

414 **10. Data availability statement**

- 415 • The mrangr package is available on CRAN (<https://cran.r-project.org/package=mrangr>). It  
416 comes with built-in function documentation and a vignette demonstrating its main  
417 functionality and workflow logic.
- 418 • The package's source code can be accessed on GitHub (<https://github.com/popecol/mrangr>)  
419 and Zenodo (<https://doi.org/10.5281/zenodo.18641951>).
- 420 • Package's website is hosted at <https://popecol.github.io/mrangr/>.
- 421 • The code and data used in the case studies are available on Zenodo  
422 (<https://doi.org/10.5281/zenodo.18643290>).

423 **11. References**

424 Adler, P. B., HilleRisLambers, J., & Levine, J. M. (2007). A niche for neutrality. *Ecology Letters*, 10(2),  
425 95–104. <https://doi.org/10.1111/j.1461-0248.2006.00996.x>

426 Chesson, P. (2000). Mechanisms of Maintenance of Species Diversity. *Annual Review of Ecology and  
427 Systematics*, 31(1), 343–366. <https://doi.org/10.1146/annurev.ecolsys.31.1.343>

428 Fallert, S., Li, L., & Cabral, J. S. (2025). metaRange: A framework to build mechanistic range models.

429 *Methods in Ecology and Evolution*, 16(1), 49–56. <https://doi.org/10.1111/2041-210X.14461>

430 Hagen, O., Flück, B., Fopp, F., Cabral, J. S., Hartig, F., Pontarp, M., Rangel, T. F., & Pellissier, L. (2021).

431 gen3sis: A general engine for eco-evolutionary simulations of the processes that shape Earth's

432 biodiversity. *PLOS Biology*, 19(7), e3001340. <https://doi.org/10.1371/journal.pbio.3001340>

433 Hijmans, R. J. (2026). *terra: Spatial Data Analysis* (Version R package version 1.8-94).

434 <https://github.com/rspatial/terra>

435 Ke, P.-J., & Letten, A. D. (2018). Coexistence theory and the frequency-dependence of priority effects.

436 *Nature Ecology & Evolution*, 2(11), 1691–1695. <https://doi.org/10.1038/s41559-018-0679-z>

437 Leibold, M. A., Chase, J. M., & Ernest, S. K. M. (2017). Community assembly and the functioning of

438 ecosystems: How metacommunity processes alter ecosystems attributes. *Ecology*, 98(4), 909–

439 919. <https://doi.org/10.1002/ecy.1697>

440 Leibold, M. A., Holyoak, M., Mouquet, N., Amarasekare, P., Chase, J. M., Hoopes, M. F., Holt, R. D.,

441 Shurin, J. B., Law, R., Tilman, D., Loreau, M., & Gonzalez, A. (2004). The metacommunity

442 concept: A framework for multi-scale community ecology. *Ecology Letters*, 7(7), 601–613.

443 <https://doi.org/10.1111/j.1461-0248.2004.00608.x>

444 Lin, J.-H., Quan, Y.-J., & Han, B.-P. (2024). MetalIBM: A Python-based library for individual-based

445 modelling of eco-evolutionary dynamics in spatial-explicit metacommunities. *Ecological*

446 *Modelling*, 492, 110730. <https://doi.org/10.1016/j.ecolmodel.2024.110730>

447 Markowska, K., Malinowska, K., & Kuczyński, L. (2025). rangr: An R package for mechanistic, spatially

448 explicit simulation of species range dynamics. *Methods in Ecology and Evolution*, 16(3), 468–

449 476. <https://doi.org/10.1111/2041-210X.14475>

450 Mouquet, N., & Loreau, M. (2003). Community Patterns in Source-Sink Metacommunities. *The*

451 *American Naturalist*, 162(5), 544–557. <https://doi.org/10.1086/378857>

452 Soberón, J. (2007). Grinnellian and Eltonian niches and geographic distributions of species. *Ecology*

453 *Letters*, 10(12), 1115–1123. <https://doi.org/10.1111/j.1461-0248.2007.01107.x>

454 Thompson, P. L., Guzman, L. M., De Meester, L., Horváth, Z., Ptacník, R., Vanschoenwinkel, B., Viana,  
455 D. S., & Chase, J. M. (2020). A process-based metacommunity framework linking local and  
456 regional scale community ecology. *Ecology Letters*, 23(9), 1314–1329.  
457 <https://doi.org/10.1111/ele.13568>

458 Tilman, D. (1994). Competition and Biodiversity in Spatially Structured Habitats. *Ecology*, 75(1), 2–16.  
459 <https://doi.org/10.2307/1939377>

460 Vellend, M. (2016). *The Theory of Ecological Communities*. Princeton University Press.  
461 <https://doi.org/10.1515/9781400883790>